Bioelectrochemistry 79 (2010) 248–253

Contents lists available at ScienceDirect

Bioelectrochemistry

journal homepage: www.elsevier.com/locate/bioelechem

Short communication

Electrochemistry and electrocatalytic of hemoglobin immobilized on FDU-15-Pt mesoporous materials

Dongxia Nie [a], Ying Liang [a], Tianshu Zhou [b], Xiaohong Li [a], Guoyue Shi [a,*], Litong Jin [a]

[a] Department of Chemistry and Shanghai Key Laboratory of Green Chemistry and Chemical Process, East China Normal University, 3663 Zhongshan Road(N), Shanghai, 200062, PR China
[b] Department of Environmental Science, East China Normal University; 3663 Zhongshan Road(N), Shanghai, 200062, PR China

ARTICLE INFO

Article history:
Received 13 July 2009
Received in revised form 24 November 2009
Accepted 8 December 2009
Available online 28 December 2009

Keywords:
Hemoglobin
FDU-Pt-15
Cyclic voltammetry
Hydrogen peroxide

ABSTRACT

In this paper, the composite films of Nafion/Hb/FDU-Pt-15/PDDA were constructed by layer-by-layer assembly technique. The FDU-15-Pt mesoporous materials were synthesized and characterized by transmission electron microscopy (TEM) and X-ray diffraction (XRD). The resulting films were verified by electrochemical impedance spectroscopy (EIS), cyclic voltammetry and UV–vis spectroscopy. The direct electrochemical and electrocatalytic properties of hemoglobin (Hb) in the Nafion/Hb/FDU-15-Pt/PDDA films were also investigated. A pair of stable and well-defined reversible redox peaks was observed and the formal potential of Hb Fe^{III}/Fe^{II} redox couple was found to be −0.324 V (vs. SCE). Based on a series of optimized conditions, the films modified electrode displayed a good electrocatalytic activity to the reduction of hydrogen peroxide (H_2O_2), which had linear current response from 2.0×10^{-6} M to 6.0×10^{-2} M with the detection limit of 1.0×10^{-6} M ($S/N=3$). The apparent Michaelis–Menten constant (K_m^{app}) was determined to be 0.15 mM in the range of lower concentration of H_2O_2. The apparent heterogeneous electron transfer rate constant (k_s) was 1.05 ± 0.03 s^{-1}. The good sensitivity, reproducibility, excellent stability and wide linear range make Nafion/Hb/FDU-15-Pt/PDDA a promising application of the preparation of third-generation biosensor.

© 2009 Elsevier B.V. All rights reserved.

1. Introduction

Direct electrochemistry of metalloproteins has attracted considerable attention for applications in mediator-free biosensors, bioreactors, and mimicking catalytic roles in living systems [1,2]. Hemoglobin (Hb), a heme protein that stores and transports oxygen in blood, consists of four polypeptides and each polypeptide chain has one electroactive heme center [3]. It is a desirable mode for function study of the redox behavior of heme proteins in biological systems because of its commercial availability and documented structure [4]. However, the inaccessibility of the redox-active heme buried within large protein matrix makes it generally difficult to establish direct electron transfer between Hb and conventional electrodes. Thus, the immobilization of redox protein on solid surface plays a key role and has aroused increasing interest among researchers [5,6].

Recently, various mesoporous materials have been used to immobilize redox protein due to their unique physical and chemical properties as well as promising applications in biological fields, such as mesoporous silicas [7], mesoporous carbon [8] and mesoporous tungsten oxide [9], etc. While the immobilization of redox protein on mesoporous materials have been realized, there were few literatures reporting the direct electrochemisty of Hb on the electrode modified with FDU-type mesoporous materials. FDU-type mesoporous materials with a phenolic resin framework is a class of advanced materials, which possess the textural porosities of mesoporous materials (well-ordered pores, large surface area and tunable structures) and simultaneously the advantages of organic polymers (high hydrophobicity, containing aromatic sections and higher stability in acid or base media in comparison to silica-based materials) [10], However, using only the FDU-type mesoporous materials as a probe for electrochemical sensing would not be adequate due to its low conductivity. To increase the conductivity, FDU-type mesoporous materials can be modified with metal nanoparticles (NPs). In fact, some noble metal NPs-functionalized FDU-type mesoporous materials, such as FDU-14-Pt [11] and FDU-15-Pd [12], have been synthesized and characterized. The unique physico-chemical characteristics and attractive catalytic performance of the resultant supported metals will endow NPs-functionalized FDU-type mesoporous materials ideal candidates as hosts for biomolecules in bioadsorption and biocatalysis fields.

In the present work, we successfully assembled Nafion/Hb/FDU-15-Pt/PDDA films modified electrode by Layer-by-Layer assembly method. The TEM and XRD experiments indicated that the FDU-15-Pt has a well-ordered mesoporous structure. A Soret band appearing in the UV–vis spectra of the protein showed that the Hb in the composite films still remained the biological activity as the native Hb. Electrochemical impedance spectroscopy (EIS) and cyclic voltammetry

* Corresponding author. Tel./fax: +86 21 62237105.
E-mail address: gyshi@chem.ecnu.edu.cn (G. Shi).

1567-5394/$ – see front matter © 2009 Elsevier B.V. All rights reserved.
doi:10.1016/j.bioelechem.2009.12.008

were utilized to monitor the layer-by-layer assembling process and the direct and reversible electrochemistry for the protein heme of Fe^{III}/Fe^{II} redox couple. The electrocatalytic reduction for hydrogen peroxide by the Nafion/Hb/FDU-15-Pt/PDDA composite electrode was also investigated in this paper.

2. Experimental

2.1. Reagents and apparatus

All chemicals were of analytical grade and were used without further purification. Hemoglobin porcine (Hb), Poly (diallyldimethylammonium) (PDDA), Nafion (5 wt.%) and Hydrogen peroxide (30%) was purchased from Sigma. 6.7 $mg \cdot mL^{-1}$ of Hb solution was prepared in 0.02 M, pH 5.5 phosphate buffer solutions (PBS), and stored at a temperature of 4 °C. The FDU-15-Pt was supplied by Shanghai Key Laboratory of Green Chemistry and Chemical Processes, Department of Chemistry, East China Normal University. The H_2O_2 solutions with different concentrations were freshly prepared for each experiment. PBS with various pH were prepared by mixed stock standard solutions of Na_2HPO_4 and NaH_2PO_4, the pH was adjusted with 0.1 M H_3PO_4 or NaOH solutions. All solutions were made from twice-distilled water. The urine samples were obtained from the local hospital and determined without any pretreatment.

The XRD patterns were collected on a Bruker D8 ADVANCE instrument using Cu-Kα radiation. The TEM images were taken on an FEI (company) Tecnai G2 Spirit at an acceleration voltage of 120 kV. UV–vis spectra of the Hb samples were measured at the wavelength ranging from 300 to 600 nm at room temperature.

2.2. Electrode fabrication

The glassy carbon electrode (GCE) was polished with 0.05-μm alumina slurry followed by thorough flushing with twice-distilled water. After that, it was sonicated in 1:1 nitric acid solution (HNO_3: H_2O, v/v), 1 M NaOH, acetone, and twice-distilled water successively and allowed to dry at room temperature.

In this paper, FDU-15-Pt mesoporous materials were used to immobilize the redox protein. Firstly, the FDU-15 was synthesized according to reference [13] and FDU-15-Pt was prepared mainly according to references [13,14]. Moreover, using the JS94G + microelectrophoresis apparatus made in China, we measured the electrokinetic potential (zeta potential) of FDU-15-Pt at different pH and found the FDU-15-Pt was most negatively charged at pH 7.6.

Nafion/Hb/FDU-15-Pt/PDDA films were deposited onto the clean, dry GCE following a layer-by-layer deposition strategy. Firstly, the clean GCE was immersed into the solution of PDDA (0.5%) for 40 min to adsorb a positively charged precursor layer of PDDA, and then the PDDA modified electrode was washed and dried under ambient conditions. Secondly, the electrode was immersed into an aqueous dispersion of FDU-15-Pt (5.0 mg/mL, 0.02 M PBS) at pH 7.6 for 40 min, where negatively charged FDU-15-Pt was adsorbed on PDDA modified GCE. Thirdly, after being washed and dried under ambient conditions, the electrode was placed in positively charged Hb solution (6.7 mg/mL, 0.02 M PBS) at pH 5.5 (pI = 7.4) for 40 min, and dried for 1 h without being washed. Finally, in order to stably immobilize the films, 3 μL of Nafion (2.5 wt.%) was dropped onto the surface of the Hb/FDU-15-Pt/PDDA modified electrode.

In order to compare FDU-15-Pt with FDU-15 mesoporous materials, the steps above were repeated to obtain Nafion/Hb/FDU-15/PDDA modified GCE.

2.3. Electrochemical characteristics of Nafion/Hb/FDU-15-Pt/PDDA modified GCE

Electrochemical experiments were carried out on a CHI660 electrochemical workstation (CH Instruments) with a bared GCE (diameter 3 mm, BAS Co., Japan) or a Nafion/Hb/FDU-15-Pt/PDDA modified GCE as the working electrode, a saturated calomel electrode (SCE) as the reference electrode and a platinum electrode as the auxiliary electrode. All electrochemical experiments were performed in 0.2 M PBS of pH 7.0. All solutions were deoxygenated by bubbling with highly pure nitrogen for at least 20 min and maintained under nitrogen atmosphere during the measurements.

3. Results and discussion

3.1. The XRD and TEM characteristics

Fig. 1A shows the wide-angle XRD of the FDU-15 and FDU-15-Pt samples, respectively. Compared with the wide-angle XRD patterns of

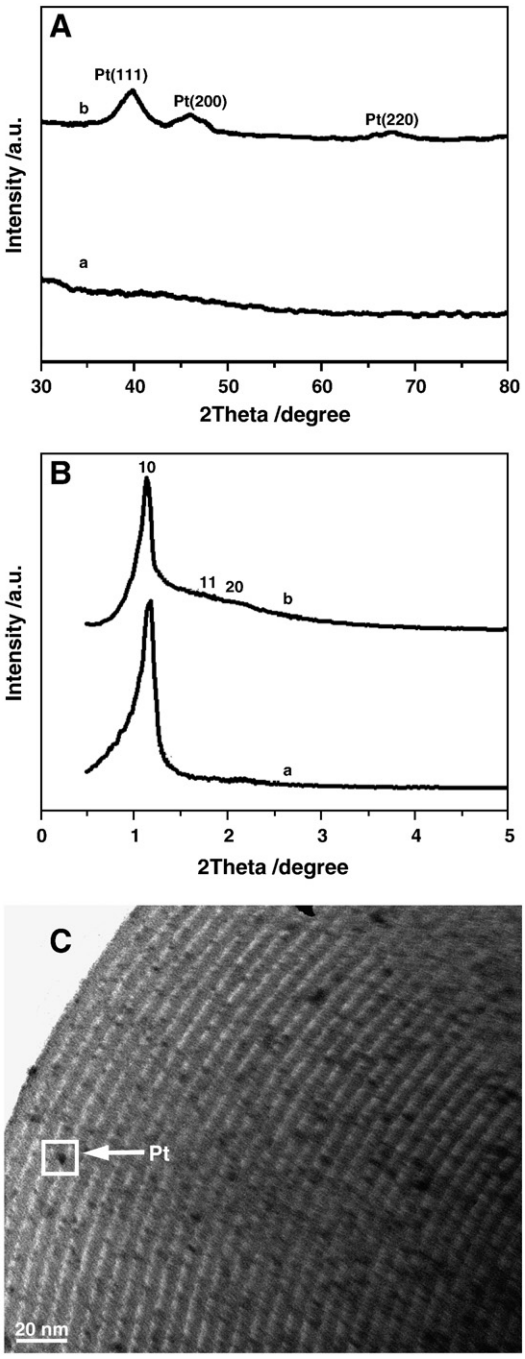

Fig. 1. (A) Wide-angle and (B) low-angel XRD patterns of the (a) FDU-15 and (b) FDU-15-Pt samples. (C) TEM image of FDU-15-Pt samples viewed along the (110) direction.

FDU-15 sample (curve a), FDU-15-Pt sample (curve b) obviously shows three Bragg reflections at $2\theta = 39.6°$, 45.8°, 67.0°, which can be indexed as the (111), (200) and (220) faces of Pt crystal by comparing with the Joint Committee on Powder Diffraction Standards (JCPDS card, NO. 04-0802), clearly indicating that the PtNPs have formed on FDU-15 support. Fig. 1B shows the low-angle XRD patterns of the FDU-15 (curve a) and FDU-15-Pt (curve b) samples. The pattern of FDU-15 exhibits an intense diffraction peak and two weak peaks that can be indexed as (10), (11), (20) reflections associated with 2D hexagonal *P6mm* [15]. Furthermore, no significant change was observed for FDU-15-Pt at a low 2θ angle, indicating that the ordered mesoporous structure remained unchanged after the incorporation of Pt nanoparticles. Fig. 1C shows the TEM image of FDU-15-Pt sample viewed along the (110) direction. The PtNPs with an average diameter of 3 nm are uniformly dispersed in the ordered mesoscopic matrix of FDU-15. The TEM image and XRD patterns are in agreement with those of previously published relative reports [10,13,14], which further confirms the FDU-15 or FDU-15-Pt synthesized in this study is indeed.

3.2. UV–vis spectroscopic characterization

Hb entrapped in the composite films was firstly investigated by spectroscopy analysis. The position of the Soret absorption band of iron heme provides information about conformation of heme proteins [16]. The Soret band shifts or disappears when Hb is denatured [17]. As can be seen from Fig. 2, Hb entrapped in the composite films has a typical characteristic Soret absorption band at 405 nm (curve b), similar to that of native Hb in pH 7.0 PBS (curve a). This reveals that Hb entrapped in the composite films has a similar structure to the native state of Hb in PBS, and retains its biological activity.

3.3. Electrochemical impedance spectroscopy characterization

Fig. 3 shows the electrochemical impedance spectroscopy (EIS) spectra observed upon the changes of surface-modified process of Hb/FDU-15-Pt/PDDA/GCE (Fig. 3A) and Hb/FDU-15/PDDA/GCE (Fig. 3B). Generally, the semicircle portion at higher frequencies corresponds to the electron transfer limited process, and the semicircle diameter of EIS equals the electron transfer resistance, R_{et} [18]. It can be seen that the semicircle diameters gradually increase corresponding to the step-by-step immobilization of PDDA, FDU-15-Pt (or FDU-15) and Hb on the electrode surface, which is the direct experimental evidence of the successful assembly of the charged films. However, there are obvious differences in impedance values between FDU-15-Pt and FDU-15 modified electrode surface. After the negatively charged FDU-15-Pt is adsorbed on the PDDA coated electrode, the R_{et} of FDU-15-Pt/PDDA/GCE changed slightly (plot c, Fig. 3A). In contrast, the corresponding R_{et} is found to dramatically increase after the FDU-15 is assembled (plot c′, Fig. 3B), which is attributed to the low conductivity of FDU-15 without encapsulated PtNPs. Since the higher hindrance effect of FDU-15 is confirmed, it is not surprised why the R_{et} of Hb/FDU-15/PDDA/GCE is more than twice as much as that of Hb/FDU-15-Pt/PDDA/GCE as given in plot d′ and d.

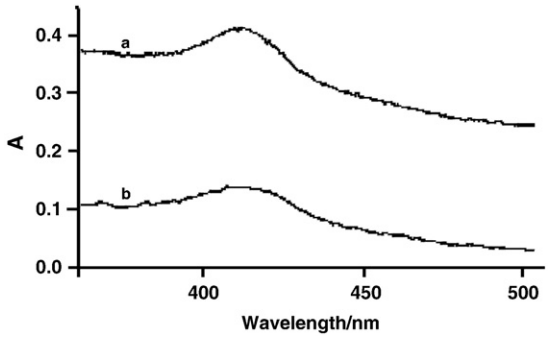

Fig. 2. UV–vis absorption spectra of (a) Hb in pH 7.0 PBS and (b) dry Nafion/Hb/FDU-15-Pt /PDDA /glassy slide.

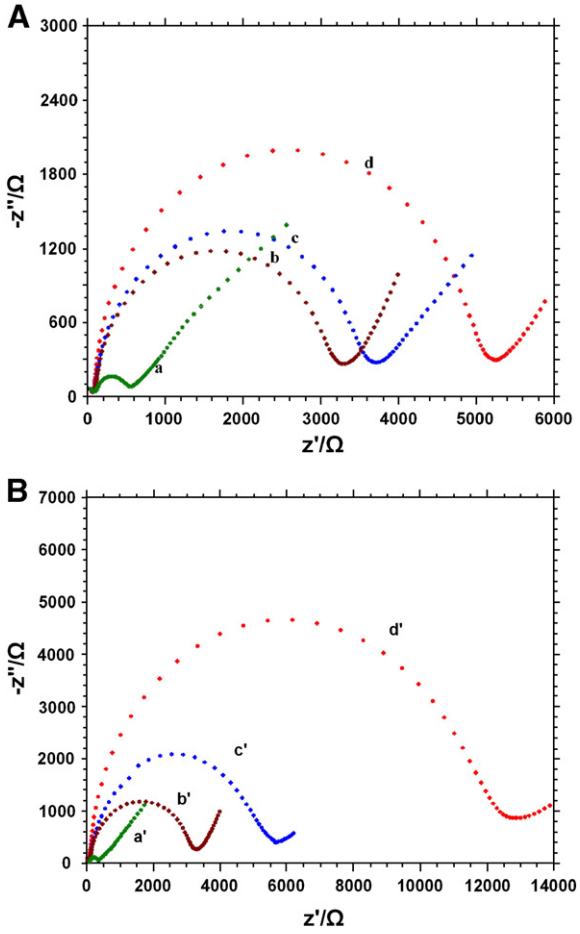

Fig. 3. (A) Nyquist plots of (a) bare GCE, (b) PDDA/GCE, (c) FDU-15-Pt/PDDA/GCE and (d) Hb/ FDU-15-Pt/PDDA/GCE. (B) Nyquist of (a′) bare GCE, (b′) PDDA/GCE, (c′) FDU-15/PDDA/GCE (d′) Hb/FDU-15/PDDA/GCE. The Nyquist plots were measured in 0.1 mol/L KCl solution containing 5.0 mM $Fe(CN)_6^{3-}/Fe(CN)_6^{4-}$.

3.4. Voltammetric characterization of Nafion/Hb/FDU-15-Pt/PDDA modified electrode

Fig. 4 shows cyclic voltammograms (CVs) recorded for (a) bare GCE, (b) Nafion/FDU-15/PDDA, (c) Nafion/FDU-15-Pt/PDDA, (d) Nafion/Hb/PDDA (e) Nafion/Hb/FDU-15/PDDA and (f) Nafion/Hb/FDU-15-Pt/PDDA modified GCE in 0.2 M, pH 7.0 PBS. A pair of well-defined reversible redox peaks is observed for Nafion/Hb/FDU-15/PDDA and Nafion/Hb/FDU-15-Pt/PDDA modified electrodes, while no obvious redox peak is observed for bare GCE, Nafion/FDU-15-Pt/PDDA and Nafion/FDU-15/PDDA modified electrodes, implying that the redox peaks comes solely from the heme Fe^{III}/Fe^{II} electron-transfer reaction in Hb. Comparatively, the Nafion/Hb/PDDA modified GCE has no redox peak as given in plot d, which presents strong evidence that FDU-15 or FDU-15-Pt mesoporous materials can facilitate the direct electron transfer between Hb and GC. Furthermore, the average surface concentration of electroactive of Hb (Γ, mol cm^{-2}) can be estimated from the charge integration of the reduction peak of the cyclic voltammograms of Nafion/Hb/FDU-15/PDDA and Nafion/Hb/FDU-15-Pt/PDDA films, using the formula of $\Gamma = Q/nFA$, where Q is the charge (C), n is the number of transfer electron, F is the Faraday constant, and A is the geometric area of the GCE (cm^{-2}). The average

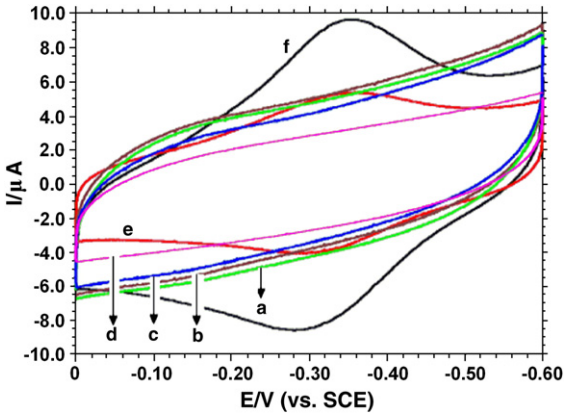

Fig. 4. Cyclic voltammograms of (a) bare GCE and (b) Nafion/FDU-15/PDDA, (c) Nafion/FDU-15-Pt/PDDA, (d) Nafion/Hb/PDDA (e) Nafion/Hb/FDU-15/PDDA, (f) Nafion/Hb/FDU-15-Pt/PDDA modified GCE in PBS solution (pH 7.0).

surface concentration of electroactive Γ of Hb of Nafion/Hb/FDU-15/PDDA and Nafion/Hb/FDU-15-Pt/PDDA films were estimated to be 3.0×10^{-11} mol cm^{-2} and 7.4×10^{-11} mol cm^{-2}, respectively, which suggested that the FDU-15 encapsulated PtNPs can act as an more efficient electron promoter for the Fe^{III}/Fe^{II} redox reaction. The results of CVs were in good agreement with the above mentioned EIS experiments. At the scan rate of 100 mV/s, the anodic peak potential ($E_{p,a}$) and the cathodic peak potential ($E_{p,c}$) of Nafion/Hb/FDU-15-Pt/PDDA films are −0.297 and −0.351 V (vs. SCE), corresponding to a peak-to-peak separation ($\triangle E_p$) of 54 mV and a formal potential (E^0) of −0.324 V calculated with $E^0 = 1/2(E_{p,a} + E_{p,c})$. The small peak-to-peak separation indicates a fast electron-transfer for Nafion/Hb/FDU-15-Pt/PDDA/GCE.

3.5. Electron transfer of Nafion/Hb/FDU-15-Pt/PDDA films

Fig. 5 shows the CVs of the Nafion/Hb/FDU-15-Pt/PDDA/GCE in PBS (pH 7.0) at different scan rates from 50 to 500 mV/s. Each voltammograms is symmetric and has a pair of well-defined redox peaks. The cathodic and anodic peak currents are linearly proportional to the scan rates in the range of 50–500 mV/s, which shows a characteristic of a surface-confined electrochemical process [19,20]. The electron-transfer rate constant (k_s) for the redox reaction of Hb was calculated using the Laviron equation [21]. The k_s value was determined to be 1.05 ± 0.03 s^{-1}, comparable to that of Hb immobilized on vaporized SiO_2 sol–gel film of 1.02 ± 0.03 s^{-1} [6], much larger than that of Hb immobilized on a poly(acrylonitrile-co-acrylic acid) film modified glassy carbon electrode of 0.58 s^{-1} [22] or immobilized on a Nafion/nano-$CaCO_3$ modified carbon ionic liquid electrode of 0.75 s^{-1} [23]. Therefore, the FDU-Pt-15 mesoporous materials facilitates the interfacial electron transfer between Hb heme center and the electrode surface.

3.6. Influence of solution pH

The pH of the buffer solution affects the electrochemical characteristics of Hb in Nafion/Hb/FDU-15-Pt/PDDA films. As is shown in Fig. 6, the CVs with stable and well-defined peaks are observed from pH 4.0 to 9.0. However, the voltammograms shift towards the negative direction with the increase of pH. The formal potentials (E^0) for the Hb heme Fe^{III}/Fe^{II} redox couple shift linearly with a slope of −49.8 mV/pH (the correlative coefficient is 0.9996), indicating that the transfer of one protein and one electron per heme group occurred according to the following reaction Eq. (1)) [24]:

$$HbFe(III) + H^+ + e^- \rightleftharpoons HbFe(II) \quad (1)$$

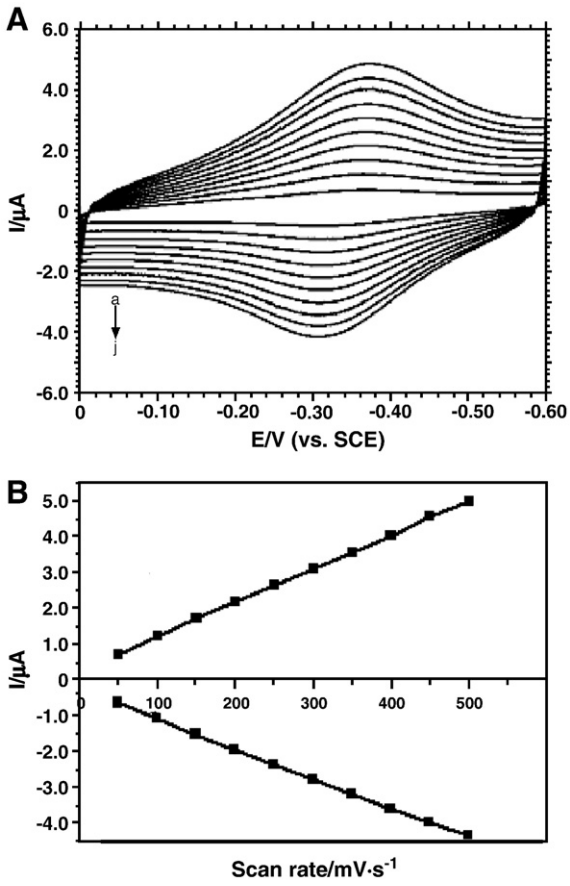

Fig. 5. (A) Cylic voltammograms of Nafion/Hb/FDU-15-Pt/PDDA electrode (a–j, from inner to outer) in pH 7.0 PBS at scan rates of (a)50, (b)100, (c)150, (d)200, (e)250, (f)300, (g)350, (h)400, (i)450, (j)500 mV/s; (B) Plot of peak current versus scan rate.

In addition, the CVs collected in the PBS of pH 4.0 before and after immersion in a PBS of pH 9.0 using the Nafion/Hb/FDU-15-Pt/PDDA/GCE were exactly the same.

3.7. Electrocatalysis of Nafion/Hb/FDU-15-Pt/PDDA films to the reduction of H_2O_2

Electrocatalytic reductions of hydrogen peroxide were examined by cyclic voltammetry using the Nafion/Hb/FDU-15-Pt/PDDA films modified electrode (figure not shown). Upon addition of H_2O_2 to the pH 7.0 PBS, the reduction peak current increased at about −0.36 V (vs. SCE) and the anodic peak current decreased dramatically, indicating

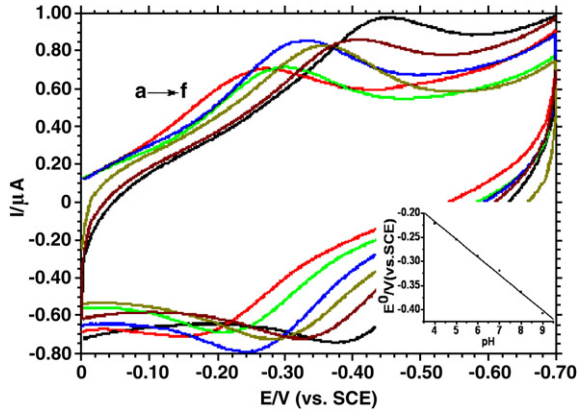

Fig. 6. CVs of Nafion/Hb/FDU-15-Pt/PDDA electrode in 0.2 M PBS with pH (a) 4.0, (b)5.0, (c) 6.0, (d)7.0, (e) 8.0, (f)9.0. Inset: plot of E^0 versus solution pH.

a typical electrocatalytic reduction process of H_2O_2. However, no direct reduction peak was observed at a bare GCE, or Nafion/FDU-15-Pt/PDDA/GCE, indicating that the reduction of H_2O_2 was catalyzed by the Hb immobilized in the Nafion/FDU-15-Pt/PDDA films.

Fig. 7 shows the current-time plot of the Nafion/Hb/FDU-15-Pt/PDDA/GCE at −0.30 V (vs. SCE) to the successive addition of H_2O_2 into pH 7.0 PBS. As H_2O_2 was added into the stirring buffer solution, the sensor could achieve 95% of the steady-state current within 5 s. The current versus added concentration of H_2O_2 was found to exhibit two linear ranges. The first range was linear between 2.0×10^{-6} M and 1.0×10^{-4} M with a correlation coefficient of 0.9977 and a slope of 16.06 nA·mM^{-1} (inset, Fig. 7A). The second range was linear from 1.0×10^{-4} M and 6.0×10^{-2} M with a correlation coefficient of 0.9996 and a slope of 2.19 nA·mM^{-1} (inset, Fig. 7B). The linear range was wider than those of Hb founded on electron tunneling of CTAB monolayer [25] or AuNPs–C@SiO_2 composite [26]. Moreover, the detection limit of 1.0×10^{-6} M was estimated at signal-to-noise ration of three ($S/N=3$), which is lower than those of some papers reported previously [9,27].

When the concentration of H_2O_2 is greater than 6.0×10^{-2} M, the current response tends to level off, indicating a typical Michaelis–Menten process. The apparent Michaelis–Menten constant (K_m^{app}), which is an indication of enzyme–substrate kinetics, can be calculated according to the Lineweaver–Burk equation [28]. In this work, when the concentration of H_2O_2 was between 2.0×10^{-6} M and 1.0×10^{-4} M, the K_m^{app} value was about 0.15 mM, much smaller than previous relative reports of 0.37 mM [1], 1.02 mM [5] and 2.87 mM [7]. Then the K_m^{app} value reached up to 25.03 mM, as the concentration of H_2O_2 ranged from 1.0×10^{-4} M to 6.0×10^{-2} M. Since the smaller

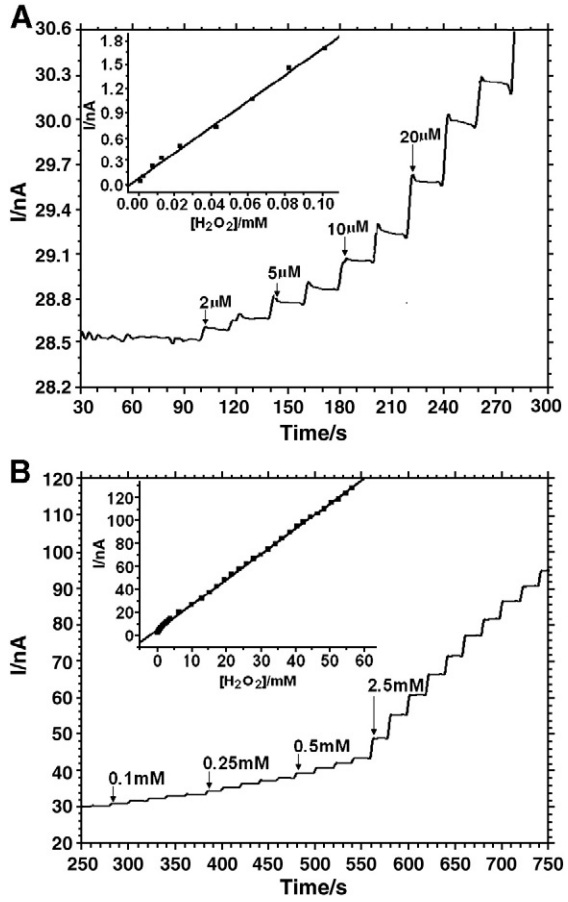

Fig. 7. Current-time responses of the Nafion/Hb/FDU-15-Pt/PDDA/GCE on successive injection of specific concentration of H_2O_2 into 0.2 M, pH 7.0 PBS, inset shows the calibration curve for H_2O_2 concentration: (A) 2.0×10^{-6} M to 1.0×10^{-4} M, (B) 1.0×10^{-4} M to 6.0×10^{-2} M. Applied potential: −0.30 V (vs. SCE).

Table 1
The detection results of real samples.

Urine sample	The amount of H_2O_2 added (μM)	The amount of H_2O_2 detected (μM)	Recovery (%)
Adult			
1	15.0	15.3	102.0
2	30.0	29.7	99.0
3	60.0	61.4	102.3
Children			
1	15.0	14.8	98.7
2	30.0	29.5	98.3
3	60.0	61.1	101.8

K_m^{app} shows the higher catalytic ability, we can conclude that the Nafion/Hb/FDU-15-Pt/PDDA films would display a higher affinity and enzymatic activity in the range of lower concentration of H_2O_2.

Additionally, to investigate the applicability of the proposed biosensor for a wider range of samples, the H_2O_2 contents in urine samples from adult and children were detected by the Nafion/Hb/FDU-15-Pt/PDDA modified electrode. None of the urine samples contained any H_2O_2, therefore they were added with three levels of H_2O_2 (15.0, 30.0 and 60.0 μM) and analyzed. As can be seen from Table 1, we achieved good recoveries of urine samples from adult and children ranging from 99.0 to 102.3% and from 98.3 to 101.8%, respectively. Therefore, the biosensor developed in this study might be a promising tool for the detection of H_2O_2 in real biological samples.

3.8. Stability and reproducibility of Nafion/Hb/FDU-15-Pt/PDDA electrode

The stability of the biosensor was investigated over a 20-day period. When the biosensor was stored dry at 4 °C and measured intermittently (twice each day), the RSD of current response to 80 μM H_2O_2 decreased about 4.0%. The good long-term stability can be attributed to the excellent biocompatibility of the composite, which can provide a favorable microenvironment for Hb to retain its bioactivity. In addition, the modified electrode also showed good reproducibility. The six electrodes, fabricated independently, showed an acceptable reproducibility in the current response to the 80 μM H_2O_2 with a RSD of 4.3%.

4. Conclusions

In this paper, we successfully fabricated the Nafion/Hb/FDU-15-Pt/PDDA modified electrode using layer-by-layer assembly technique. The FDU-15-Pt mesoporous materials, which possess unique physicochemical characteristics and attractive catalytic performance of the encapsulated PtNPs, can efficiently improve the electron transfer between Hb and electrode surface. The apparent heterogeneous electron transfer rate constant (k_s) of Hb was found to be 1.05 ± 0.03 s^{-1}. Additionally, the immobilized Hb still retained its native conformation and displayed an excellent eletrocatalytical activity to the reduction of H_2O_2 with the detection limit of 1.0×10^{-6} M ($S/N=3$). The apparent Michaelis–Menten constant (K_m^{app}) was determined to be 0.15 mM in the range of lower concentration of H_2O_2. Therefore the Nafion/Hb/FDU-15-Pt/PDDA films are promising in the fabrication of the third-generation biosensors based on the direct electrochemistry of enzymes.

Acknowledgements

This work is supported by the National Natural Science Foundation of China (No 20675032, 20703018), Program for New Century Excellent Talents in University (NCET-07-0293), the project

sponsored by the Scientific Research Foundation of State Education Ministry for the Returned Overseas Chinese Scholars and the funding from Shanghai Key Laboratory of Green Chemistry and Chemical Processes.

References

[1] Z.Y. Sun, Y.Q. Li, T.S. Zhou, Y. Liu, G.Y. Shi, L.T. Jin, Direct electron transfer and electrocatalysis of hemoglobin in layer-by-layer films assembled with Al-MSU-S particles, Talanta 74 (2008) 1692–1698.
[2] F.A. Armstrong, G.S. Wilson, Recent developments in faradaic bioelectrochemistry, Electrochim. Acta 45 (2000) 2623–2645.
[3] Y. Sun, X. Liu, C. Fan, W. Zhang, G. Li, Electrochemical investigation of the chloride effect on hemoglobin, Bioelectrochemistry 64 (2004) 23–27.
[4] H. Ohno, Electron transfer reaction of heme-proteins in ion conductive polymer matrix, Electrochim. Acta 43 (1998) 1581–1587.
[5] M.C. Liu, G.H. Zhao, K.J. Zhao, X.L. Tong, Y.T. Tang, Direct electrochemistry of hemoglobin at vertically-aligned self-doping TiO_2 nanotubes: a mediator-free and biomolecule-substantive electrochemical interface, Electrochem. Commun. 11 (2009) 1397–1400.
[6] G.Y. Shi, Z.Y. Sun, M.C. Liu, L. Zhang, Y. Liu, Y.H. Qu, L.T. Jin, Electrochemistry and electrocatalytic properties of hemoglobin in layer-by-layer films of SiO_2 with vapor-surface sol–gel deposition, Anal. Chem. 79 (2007) 3581–3588.
[7] Y.Z. Xian, Y. Xian, L.H. Zhou, F.H. Wu, Y. Ling, L.T. Jin, Encapsulation hemoglobin in ordered mesoporous silicas: Influence factors for immobilization and bioelectrochemistry, Electrochem. Commun. 9 (2007) 142–148.
[8] C.P. You, X.W. Yan, J.L. Kong, D.Y. Zhao, B.H. Liu, Direct electrochemistry of myoglobin based on bicontinuous gyroidal mesoporous carbon matrix, Electrochem. Commun. 10 (2008) 1864–1867.
[9] J.J. Feng, J.J. Xu, H.Y. Chen, Direct electron transfer and electrocatalysis of hemoglobin adsorbed onto electrodeposited mesoporous tungsten oxide, Electrochem. Commun. 8 (2006) 77–82.
[10] Y. Yan, J. Wei, F.Q. Zhang, Y. Meng, B. Tu, D.Y. Zhao, The pore structure evolution and stability of mesoporous carbon FDU-15 under CO_2, O_2 or water vapor atmospheres, Micropor. Mesopor. Mater. 113 (2008) 305–314.
[11] X.H. Li, L.Y. Shen, L.Y. Song, H.N. Wang, H.H. Wu, Y.M. Liu, P. Wu, Efficient hydrogenation of benzaldehydes over mesopolymer-entrapped Pt nanoparticles in water, Chem. Asian J. 4 (2009) 699–706.
[12] R. Xing, Y.M. Liu, H.H. Wu, X.H. Li, M.Y. He, P. Wu, Preparation of active and robust palladium nanoparticle catalysts stabilized by diamine-functionalized mesoporous polymers, Chem. Commun. 47 (2008) 6297–6299.
[13] Y. Meng, D. Gu, F.Q. Zhang, Y.F. Shi, H.F. Yang, Z. Li, C.Z. Yu, B. Tu, D.Y. Zhao, Ordered mesoporous polymers and homologous carbon frameworks: amphiphilic surfactant templating and direct transformation, Angew. Chem. Int. Ed. 44 (2005) 7053–7059.
[14] X.H. Li, Y.L. Shen, R. Xing, Y.M. Liu, H.H. Wu, M.Y. He, P. Wu, Effective and reusable Pt catalysts supported on periodic mesoporous resols for chiral hydrogenation, Catal. Lett. 122 (2008) 325–329.
[15] D.Y. Zhao, J.L. Feng, Q.S. Huo, N. Melosh, G.H. Fredrickson, B.F. Chmelka, G.D. Stucky, Triblock copolymer syntheses of mesoporous silica with periodic 50 to 300 angstrom pores, Science 279 (1998) 548–552.
[16] Y. Liu, W.Z. Zhang, T.J. Pinnavaia, Steam-stable aluminosilicate mesostructures assembled from zeolite type Y seeds, J. Am. Chem. Soc. 122 (2000) 8791–8792.
[17] A.-E.F. Nassar, W.S. Willis, J.F. Rusling, Electron transfer from electrodes to myoglobin: facilitated in surfactant films and blocked by-adsorbed biomacromolecules, Anal. Chem. 67 (1995) 2386–2392.
[18] D. Chen, G. Wang, W. Lua, H. Zhang, J.H. Li, Photoelectrochemical study of organic–inorganic hybrid thin films via electrostatic layer-by-layer assembly, Electrochem. Commun. 9 (2007) 2151–2156.
[19] H.C. Yoon, M.Y. Hong, H.S. Kim, Functionalization of a poly(amidoamine) dendrimer with ferrocenyls and its application to the construction of a reagentless enzyme electrode, Anal. Chem. 72 (2000) 4420–4427.
[20] Z.H. Dai, S.Q. Liu, H.X. Ju, H.Y. Chen, Direct electron transfer and enzymatic activity of hemoglobin in a hexagonal mesoporous silica matrix, Biosens. Bioelectron. 19 (2004) 861–867.
[21] E.J. Laviron, General expression of the linear potential sweep voltammogram in the case of diffusionless electrochemical systems, Electroanal. Chem. 101 (1979) 19–28.
[22] D. Shan, G.X. Cheng, D.B. Zhu, H.G. Xue, S. Cosnier, S.N. Ding, Direct electrochemistry of hemoglobin in poly(acrylonitrile-co-acrylic acid) and its catalysis to H_2O_2, Sensors Actuators B 137 (2009) 259–265.
[23] W. Sun, R.F. Gao, K. Jiao, Electrochemistry and electrocatalysis of hemoglobin in Nafion/nano-$CaCO_3$ film on a new ionic liquid $BPPF_6$ modified carbon paste electrode, J. Phys. Chem. B 111 (2007) 4560–4567.
[24] H.H. Liu, Z.Q. Tian, Z.X. Lu, Z.L. Zhang, M. Zhang, D.W. Pang, Direct electrochemistry and electrocatalysis of heme-proteins entrapped in agarose hydrogel films, Biosens. Bioelectron. 20 (2004) 294–304.
[25] Q. Lu, C.G. Hu, R. Cui, S.S. Hu, Direct electron transfer of hemoglobin founded on electron tunneling of CTAB monolayer, J. Phys. Chem. B 111 (2007) 9808–9813.
[26] Y.Y. Wang, X.J. Chen, J.J. Zhu, Fabrication of a novel hydrogen peroxide biosensor based on the AuNPs–C@SiO_2 composite, Electrochem. Commun. 11 (2009) 323–326.
[27] A. Safavi, N. Maleki, O. Moradlou, M. Sorouri, Direct electrochemistry of hemoglobin and its electrocatalytic effect based on its direct immobilization on carbon ionic liquid electrode, Electrochem. Commun. 10 (2008) 420–423.
[28] R.A. Kamin, G.S. Wilson, Rotating ring-disk enzyme electrode for biocatalysis kinetic studies and characterization of the immobilized enzyme layer, Anal. Chem. 52 (1980) 1198–1205.